

Published in final edited form as:

J Neuropathol Exp Neurol. 2013 April ; 72(4): 272–285. doi:10.1097/NEN.0b013e318288a8dd.

Rapid β -Amyloid Deposition and Cognitive Impairment after Cholinergic Denervation in APP/PS1 Mice

Juan Jose Ramos-Rodriguez, BSci^{1,*}, Mar Pacheco-Herrero, BSci^{1,*}, Diana Thyssen, BSci², Maria Isabel Murillo-Carretero, PhD¹, Esther Berrocoso, PhD^{3,4}, Tara L. Spires-Jones, DPhil², Brian J. Bacskai, PhD², and Monica Garcia-Alloza, PhD¹

¹Division of Physiology, School of Medicine, University of Cadiz, Spain.

²Department of Neurology, MGH Harvard Medical School, Charlestown, MA.

³Department of Neuroscience, School of Medicine, University of Cadiz, Spain.

⁴Centro de Investigación Biomédica en Red de Salud Mental (CIBERSAM), Instituto de Salud Carlos III, Madrid, Spain.

Abstract

Although extensive evidence supports the role of amyloid- β (A β) in Alzheimer disease (AD), the neurotoxic mechanisms underlying AD pathogenesis are not understood. On the other hand, neuronal loss is the pathological feature that best correlates with cognitive impairment. We hypothesized that cholinergic neurodegeneration may lead to A β deposition and tested this by inducing selective cholinergic lesions in APP^{swe}/PS1^{dE9} mice with murine p75^{NTR} saporin (mu p75-SAP). Intracerebroventricular lesions that removed ~50% of cholinergic innervation to the cortex and hippocampus were induced in animals with incipient (~3 months) and marked (~7 months of age) A β deposition. Cranial windows were implanted and A β deposition was monitored in vivo using multiphoton microscopy. A β deposition was increased as soon as 7 days after the lesion and this effect was maintained up to 3 months later. Postmortem studies using immunohistochemistry with an anti-A β antibody corroborated these findings in both cerebral cortex and hippocampus. Tau phosphorylation was also significantly increased after the lesions. Cholinergic denervation resulted in early memory impairment at 3 months of age that worsened with age (~7 months); there was a synergistic effect between cholinergic denervation and the presence of APP/PS1 transgenes. Altogether, our data suggest that cholinergic denervation may trigger A β deposition and synergistically contribute to cognitive impairment in AD patients.

Keywords

β -amyloid; Alzheimer disease; Basal forebrain; Cholinergic system; Murine p75^{NTR} saporin; Senile plaques

Send correspondence and reprint requests to: Monica Garcia-Alloza, PhD, Division of Physiology, School of Medicine, University of Cadiz, Plaza Fragela 9, 4 piso, 410, Cadiz (11003), Spain. Tel: +34 956015252. monica.garcia@uca.es.

*Equally contributing authors.

Publisher's Disclaimer: This is a PDF file of an unedited manuscript that has been accepted for publication. As a service to our customers we are providing this early version of the manuscript. The manuscript will undergo copyediting, typesetting, and review of the resulting proof before it is published in its final citable form. Please note that during the production process errors may be discovered which could affect the content, and all legal disclaimers that apply to the journal pertain.

INTRODUCTION

Alzheimer disease (AD) is the most common cause of dementia among elderly people. Although the ultimate neurotoxic mechanisms have not been completely elucidated, major hallmarks of the disease include senile plaques (SPs), mainly composed of amyloid- β (A β), neurofibrillary tangles, consisting of aggregated hyperphosphorylated tau protein, and neuronal loss (1, 2). Specifically, cholinergic cell loss in the basal forebrain (BFB), the major source of cortical and hippocampal cholinergic projections, seems to correlate better than SPs and tangles with clinical dementia in AD (3). A close relationship has also been documented between A β deposition and neurodegeneration, and previous studies have shown that senile plaque (SP) deposition can lead to neuronal abnormalities (4, 5). Cholinergic neurons seem to be particularly highly susceptible in AD (6), and experimental cholinergic denervation may interfere with amyloid precursor protein (APP) (6). Moreover, cholinergic loss might exacerbate cognitive impairment in experimental AD (7). However, to our knowledge, whether specific cholinergic neurodegeneration leads to SP deposition in innervated areas remains unclear.

Different transgenic mice, including APP^{swe}/PS1^{dE9} mice, have been developed to study the etiology, evolution and new therapeutic alternatives of AD. These mice are widely used by the scientific community because they show SP deposition at 4 to 6 months of age (8, 9) as well as learning and memory deficits by 8 months (10). As in other AD transgenic models, however, they do not reproduce the complexity of the illness because they do not show overt neuronal loss or tau pathology (11). Although previous studies have found evidence of cholinergic terminal abnormalities in this and other transgenic AD mouse models, BFB cholinergic somata seem to be preserved (11, 12). Therefore, producing an animal model that shows both specific neuronal loss and A β deposition could help elucidate the relationship between SPs and cholinergic denervation observed in human AD. In order to develop such a model, we selectively removed BFB cholinergic neurons in APP^{swe}/PS1^{dE9} mice using murine p75^{NTR} saporin (mu p75-SAP), a highly specific cholinergic immunotoxin that selectively targets the mouse p75^{NTR} receptor (7). By injecting the immunotoxin into the lateral ventricles, we were able to reach the BFB, including the nucleus basalis of Meynert and medial septum, major sources of cortical and hippocampal cholinergic innervation. We used *in vivo* multiphoton microscopy (MPM) to assess acute and long-term SP deposition in young and adult APP^{swe}/PS1^{dE9} mice upon BFB cholinergic denervation and assessed learning and memory deficits in the mice.

MATERIALS AND METHODS

Animals and Cholinergic Denervation

APP^{swe}/PS1^{dE9} mice were obtained from Jackson Laboratory (Bar Harbor, ME). Animals were aged to ~3 and ~7 months of age and experimental procedures were approved by the Massachusetts General Hospital and the Animal Care and Use Committee of the University of Cadiz, in accordance with the Guidelines for Care and Use of experimental animals (European Commission Directive 86/609/CEE and Spanish Royal Decree 1201/2005).

To remove cholinergic innervation to the cortex and hippocampus, the BFB was exposed to the cholinergic specific immunotoxin mu p75-SAP (Advanced Targeting Systems, San Diego, CA), as previously described (11, 13, 14). Vehicle-injected animals were used as controls (Sham). Acute lesions were performed in ~3-month-old (Wild type (Wt) Sham n = 16, Wt Sap n = 13, APP/PS1 Sham n = 17, APP/PS1 Sap n = 12) and ~7-month-old mice (Wt Sham n = 19, Wt Sap n = 15, APP/PS1 Sham n = 17, APP/PS1 Sap n = 19). To determine whether lesions were completely established 1 week after the injection (when animals were tested for *in vivo* A β deposition and learning and memory abilities), a group of

7-month-old mice (n = 3) was lesioned and killed 7 days later to determine the extent of the lesion at that time. A group of lesioned ~3-month-old mice (Wt Sham n = 18, Wt Sap n = 13, APP/PS1 Sham n = 17, APP/PS1 Sap n = 19) was allowed to age to assess long-term lesion effects. Long-term lesioned mice were tested for A β deposition and behavioral impairment immediately before sacrifice at 7 months of age. Behavioral tests were performed on all animals that did not undergo in vivo imaging. For postmortem studies, half of the brains were fixed in paraformaldehyde (PFA) for immunohistochemistry studies and the rest were fresh frozen for biochemical determinations.

Briefly, mice were anesthetized with a subepidermal injection of xylazine (10 mg/kg) (Rompun 2%, Bayer Pharma, San Juan Despi, Spain) and an i.p. injection of ketamine (100 mg/kg) (Imalgene 500, Merial, Tarragona, Spain) and placed in a stereotaxic device. Lesions of the BFB were performed by bilateral intracerebroventricular injections (AP -0.6 mm; ML \pm 1.2 mm; DV +2 mm from bregma) of the immunotoxin mu p75-SAP (1-1.2 μ g/ μ l), diluted in phosphate buffered saline. We injected 1 μ l/hemisphere using a Hamilton syringe at a constant flow rate of 0.1 μ l/minute for 10 minutes; a delay of 10 minutes was allowed before complete retraction of the needle to minimize aspiration of the toxin. Sham operated mice followed the same procedure but only phosphate buffered saline was injected.

Actimetry and New Object Discrimination Tests

Episodic memory in young and older mice treated with mu p75-SAP was assessed with the New Object Discrimination (NOD) test as previously described with minor modifications (15). Acutely lesioned mice, ~3 months old (APP/PS1 Sap n = 10, APP/PS1 Sham n = 9, Wt Sap n = 9, Wt Sham n = 9) and ~7 months old (APP/PS1 Sap n = 8, APP/PS1 Sham n = 8, Wt Sap n = 9, Wt Sham n = 14) mice were tested 7 days after the lesions, when cholinergic denervation was established (16-18). Long-term mu p75-SAP-treated mice were evaluated at the age of 7 months (APP/PS1 Sap n = 7, APP/PS1 Sham n = 9, Wt Sap n = 6, Wt Sham n = 17), before death. We assessed locomotor activity of all the animals in the study by measuring the distance travelled by mice for 30 minutes prior to the commencement of the NOD test. Testing was conducted for 3 consecutive days as follows: On day 1, mice were habituated for 30 minutes to a transparent rectangular box (22 cm long \times 44 cm width \times 40 cm high), where the procedure takes place. On day 2, animals were exposed to 2 objects for habituation purposes that were not used again during the object exploration task. On day 3, each mouse received 2 sample trials and a test trial. On the first sample trial, mice were placed in the center of the box containing 3 copies of a novel object arranged in a triangle-shaped spatial configuration and allowed to explore them for 5 minutes. After a delay of 30 minutes, mice received a second sample trial with 4 novel objects, arranged in a quadratic-shaped spatial configuration for 5 minutes. After a delay of 30 minutes, mice received a test trial with 2 copies of the object from sample trial 2 placed at the same position ("recent non-displaced" objects) and 2 copies of the object from sample trial 1 ("old" objects) placed one of them at the same position ("old non-displaced" object) and the other in a new position ("old displaced" object). Integrated memory for "what," "where," and "when" were analyzed as previously described (15): "What" was defined as the difference in time exploring familiar and recent objects; "where" was defined as the difference in time exploring displaced and non-displaced objects; and "when" was defined as the difference between time exploring "old non-displaced" and "recent non-displaced" objects (15).

Morris Water Maze

Learning and memory abilities were further analyzed in animals that underwent the NOD test, using the Morris Water Maze test as previously described with minor modifications (19). All groups under study, i.e. those with 3-month-old acute lesions (APP/PS1 Sap n = 11, APP/PS1 Sham n = 10, Wt Sap n = 8, Wt Sham n = 9), 7-month-old acute lesions (APP/PS1

Sap n = 9, APP/PS1 Sham n = 11, Wt Sap n = 11, Wt Sham n = 18), and 7-month-old long-term lesions (APP/PS1 Sap n = 7, APP/PS1 Sham n = 8, Wt Sap n = 6, Wt Sham n = 17) were tested. Experiments commenced the day after the conclusion of the NOD test for all the groups. The maze consisted of a round tank of water (0.95 m in diameter) with 4 equal virtual quadrants indicated with geometric cues mounted on the walls. An escape platform was 2 to 3 cm below the water surface and was camouflaged with calcium carbonate to cloud the water. Water temperature was $21 \pm 1^\circ\text{C}$. A camera was mounted above the maze and attached to a computer with the software Smart (Panlab, Barcelona, Spain). Testing was conducted in 2 phases: acquisition and retention. Acquisition consisted of 4 trials/day for 4 days with the platform submerged. During this phase the platform was located in quadrant 2. The time limit was 60 seconds/trial with an intertrial interval of 10 minutes. If the animal did not find the platform it was placed on it for 10 seconds. The retention phase began a day after acquisition testing. It consisted of a single trial with the platform removed. Average times to locate the platform during the acquisition phase, as well as the percentage of total time spent in each quadrant during the retention phase, were determined.

In Vivo Assessment of SP Deposition Using MPM

To perform in vivo imaging, cranial windows were placed immediately after surgery, as previously described with minor modifications (20). Briefly, a 6-mm craniotomy was drilled between Bregma and Lambda sutures and a glass coverslip was attached with dental cement. Fluorescent angiograms were included to facilitate finding the same cerebral regions between sessions using fluorescent injections in the lateral tail vein with Texas Red Dextran 70 KD (Invitrogen, Carlsbad, CA). Methoxy-XO4 (5 mg/kg), a Congo red derivative that crosses the blood brain barrier and binds fibrillar A β (21), was injected i.p. the day before the imaging session to visualize SPs. Young mice (3 months old, APP/PS1 Sap n = 5, APP/PS1 Sham n = 5) and older mice (7 months old, APP/PS1 Sap n = 4, APP/PS1 Sham n = 4) were imaged immediately after surgery (day 0), allowed to recover and imaged again on day 7 and day 14. Long-term denervation experiments were also carried out in mice with lesions performed at 3 months and imaged up to 3.5 months later (at ~7 months) (APP/PS1 Sap n = 4, APP/PS1 Sham n = 4). The images were obtained with a multiphoton microscope Bio-Rad1024 (Bio-Rad, Hercules, CA) where two-photon fluorescence was generated with 800-nm excitation from a Ti:Sapphire laser (Mai Tai; Spectra Physics, Mountain View, CA), as previously described (8, 22). External detectors collected emitted fluorescent light from methoxy-XO4 and Texas red. Multiple series were imaged and leptomeningeal cerebral vessels were used as local markers. *In vivo* imaging was done using a 20 \times water immersion objective (Olympus, NA = 0.95, 615 \times 615 μm ; z-step, 5 μm , depth, approximately 200 μm). Maximum intensity projections of z-series were generated using the Image J software. Stacks were used to measure plaque size and number (23). Senile plaque size was measured by thresholding, segmenting, and measuring the blue fluorescence channel.

Acetyl Cholinesterase Determination

Extension and selectivity of the lesions were assessed by acetyl cholinesterase (AChE) assay as previously described with minor modifications (24). Cortex, hippocampus and striatum from 3 months acute lesioned mice (APP/PS1 Sap n = 6, APP/PS1 Sham n = 6, Wt Sap n = 4, Wt Sham n = 4) 7 months acute lesioned mice (APP/PS1 Sap n = 9, APP/PS1 Sham n = 13, Wt Sap n = 13, Wt Sham n = 19) and 7 months long-term lesioned mice (APP/PS1 Sap n = 5, APP/PS1 Sham n = 11, Wt Sap n = 11, Wt Sham n = 19) were homogenized in 30 volumes of 75 mM saline phosphate buffer (pH 7.4). Briefly, 111 μl of acetylthiocholine iodide (Sigma, St. Louis, MO) 0.3 mM, 28 μl of saline phosphate buffer 100 mM (pH 7.4) and 7 μl of tissue homogenate were incubated in a 96-well plate for 8 minutes at 37 $^\circ\text{C}$. The reaction was then terminated by adding 28 μl of sodium dodecyl sulphate (Sigma) 0.2% (w/v) and 28 μl of 5.5'-dithio-(2-bisnitrobenzoico) (Sigma) 0.5% (w/v). Color was measured

spectrophotometrically at 450 nm (MQX200R2, Biotek instruments, Burlington VT). All samples were assayed in duplicate. Results were expressed as percentage of those obtained for Wt Sham animals.

A β , Choline Acetyltransferase and Parvalbumin Immunohistochemistry

Both acute and long-term mu p75-SAP-treated mice were assessed postmortem for A β burden in cortex and hippocampus at 3 months (APP/PS1 Sap n = 4, APP/PS1 Sham n = 5) 7 months acute (APP/PS1 Sap n = 4, APP/PS1 Sham n = 4) and 7 months long-term (APP/PS1 Sap n = 4, APP/PS1 Sham n = 4). Immunohistochemistry for A β was performed as previously described (25) with minor modifications. PFA-fixed 30- μ m sections were washed in TBS and pre-treated with 70% formic acid for 30 minutes at room temperature (RT). Sections were blocked in 5% normal goat serum with 0.5% Triton-X100 for 1 hour. Sections were rinsed in TBS and incubated with anti- β A1–16 antibody 1:600 (Millipore, Billerica, MA) in 1% normal goat serum overnight at 4°C. After washing in TBS, sections were incubated with anti-mouse Alexa Fluor 594 1:200 (Invitrogen) for 1 hour. Senile plaques were stained with thioflavin S 0.1% (w/v) for 10 minutes and washed in 80% ethanol and dH₂O. The number of plaques, plaque size and plaque burden (expressed as percentage of analyzed area) were calculated using Adobe Photoshop and Image J software for each age group under study.

Because AChE is not an exclusive cholinergic marker and can also be detected in synaptic clefts and cholinceptive neurons, we further assessed cholinergic denervation of the BFB by immunohistochemistry for choline acetyltransferase (ChAT) in these regions (n = 3/ group). Although it is mainly cholinergic, the BFB also contains other neuronal populations. To assess possible nonspecific damage of γ -aminobutyric acid-releasing (GABAergic) neurons after mu p75-SAP lesions we included double immunostaining for parvalbumin. Sections were washed in TBS and incubated in 70% formic acid at 37°C for 30 minutes. After washing, sections were blocked in 5% bovine serum albumin and 0.1% triton-X for 1 hour at RT. Tissue was incubated with primary antibodies anti-ChAT (1:1000) and anti-parvalbumin (1:1000) (Millipore) in 2.5% bovine serum albumin and 0.1% triton-X for 72 hours at 4°C. After washing, sections were then incubated in Alexa Fluor 594 anti-rabbit and Alexa Fluor 488 anti-mouse 1:1000 (Invitrogen) at RT for 1 hour. Sections were mounted, coverslipped and photographed with a fluorescence microscope (Olympus Bc60, Tokyo, Japan).

Tau and Phospho-tau Levels

Cortical samples from mu p75-SAP-treated and Sham mice 3 months acute (APP/PS1 Sap n = 8, APP/PS1 Sham n = 8, Wt Sap n = 8, Wt Sham n = 8), 7 months acute (APP/PS1 Sap n = 6, APP/PS1 Sham n = 6, Wt Sap n = 6, Wt Sham n = 5), and 7 months long-term (APP/PS1 Sap n = 8, APP/PS1 Sham n = 8, Wt Sap n = 8, Wt Sham n = 8) were homogenized in lysis buffer (Cell Signaling, Beverly, MA) and supplemented with a protease and phosphatase inhibitor cocktail (Sigma). The homogenates were sonicated and centrifuged at 4°C for 5 minutes at 15,000 \times g. Supernatants were collected and protein concentration determined using the Bradford protein assay (BioRad, Munich, Germany). Proteins were separated on 10% acrylamide-bisacrylamide gels, followed by electrophoretic transfer to PVDF membranes (Schleicher & Schuell, Keene, NH). Membranes were then immersed in blocking buffer (Invitrogen) for 1 hour and incubated overnight at 4°C with primary antibodies for total tau (1:1000) (DAKO, Glostrup, Denmark). Membranes were washed and then incubated with chemiluminescent immunodetection system for mouse and rabbit primary antibodies respectively (Invitrogen). Membranes were washed and signal was detected using Novex AP Chemiluminescent Substrate (Invitrogen) and Kodak Biomax Light Film (Sigma). After stripping, membranes were incubated with anti-phospho-tau

antibody (1:1000) (clone AT8, Fisher Scientific, Waltham, MA). Immunoblots were semi-quantified by measuring the optical density of each protein band on scanned film using the ImageJ software. Each band was normalized to α -tubulin optical density and phospho tau/total tau ratio was represented as percentage of Wt Sham mice values.

RESULTS

Intracerebroventricular Infusion of the Immunotoxin mu p75-SAP Results in Cortical and Hippocampal Cholinergic Depletion

Wt and APP/PS1 mice received bilateral injections of the immunotoxin mu p75-SAP into the lateral ventricles. This procedure allows the immunotoxin to reach BFB areas, including the nucleus basalis of Meynert and the medial septum, resulting in specific degeneration of cholinergic neurons in these areas (7). To confirm that mu p75-SAP infusions resulted in cholinergic denervation, we measured AChE activity in cortex and hippocampus, the main projection areas of BFB cholinergic neurons. Because behavioral tests and in vivo MPM were started 1 week after the lesions, we assessed AChE activity in a separate group of mice at this time point; we observed a similar profile to that observed at 2 weeks.

At 1 week post-lesion, AChE activity, expressed as percentage of Wt Sham values, was significantly reduced in cortex of Wt and APP/PS1 lesioned mice (Wt Sham: 100.00 ± 2.20 , Wt SAP: 57.45 ± 6.47 , APP/PS1 Sham: 90.80 ± 9.79 , APP/PS1 SAP: 55.27 ± 7.76 , [$F_{(3,31)}=7.097$, ** $p=0.01$ vs. Wt Sham]). A similar profile was observed in the hippocampus (Wt Sham: 100.00 ± 15.07 , Wt SAP: 45.81 ± 3.40 , APP/PS1 Sham: 88.20 ± 4.67 , APP/PS1 SAP: 57.38 ± 3.48 , [$F_{(3,32)}=15.309$, ** $p < 0.01$ vs. Wt Sham]). Cholinergic activity in the striatum was preserved (Wt Sham: 100.00 ± 12.82 , Wt SAP: 84.86 ± 10.90 , APP/PS1 Sham: 106.74 ± 11.62 , APP/PS1 SAP: 84.34 ± 2.60 , [$F_{(3,31)}=1.612$, $p=0.206$]). When AChE activity was assessed 2 weeks after the lesion (when behavioral assessment was completed), both Wt and APP/PS1 denervated mice showed a ~40% to 50% reduction of AChE activity in cortex and hippocampus, whereas areas not innervated by the BFB (e.g. striatum) were intact, indicating selectivity of the lesion (Table). We observed a slight, non-significant, reduction in AChE activity in Sham transgenic mice, compared to Wt Sham, suggesting some cholinergic degeneration in this animal model, as previously described (11). Further confirmation of BFB cholinergic loss was obtained using immunohistochemistry for ChAT in the medial septum. There was a reduction in ChAT staining in mu p75-SAP-infused animals, whereas parvalbumin-positive neurons were preserved in lesioned mice, supporting the specificity of the cholinergic denervation (Fig. 1).

Effect of Cholinergic Denervation on Cognition

Prior to cognition studies, motor function integrity was assessed in all animal groups. The actimetry test revealed that distance travelled and speed were similar in all groups (3 and 7 months of age) (data not shown). This indicated that motor disturbances were absent, that mu p75-SAP-induced lesions were limited to the denervated areas, and that Purkinje cells were likely preserved. We performed NOD tests to evaluate episodic memory in Wt and APP/PS1 mice with or without cholinergic denervation. The NOD task test assesses episodic memory and is a very sensitive tool to detect early memory alterations in animal models. There was general impairment in episodic memory in all denervated mice at 3 and 7 months of age (both those that were acutely and those that were chronically lesioned). All 3 parameters analyzed (“what,” “where,” and “when”) were significantly impaired in mu p75-SAP-treated mice and there was also an overall worsened performance associated with aging. In aged mice (7 months old) vs. 3 months old mice a significant age X transgene effect for all paradigms (what: [$F_{(2,1)}=12.243$, $p < 0.01$], where: [$F_{(2,1)}=13.81$, $p=0.023$], when: [$F_{(2,1)}=19.710$, $p < 0.01$]), supporting an age effect on episodic memory. There was a

significant effect in young transgenic mice (3 months of age) (Fig. 2), independent of the presence of a cholinergic lesion, whereas at 7 months of age, the cholinergic lesion worsened the performance of transgenic lesioned mice. Statistical analysis included one-way ANOVA followed by Tukey-b or Tamhane tests, as required for each variable. Assessment of the difference in time exploring familiar and recent objects (what) indicated significant impairment in 3-month-old transgenic mice without a significant effect of the mu p75-SAP lesions [$F_{(3,107)}=21.208$, ** $p < 0.01$ vs. Wt mice] (Fig. 2). In older mice (7 months of age), we observed some effect on episodic memory and a significantly worse performance of transgenic lesioned mice vs. the other groups in relation to parameter "what" [$F_{(3,155)}=10.39$, * $p < 0.01$ vs. other groups] (Fig. 2). A similar profile was observed in long-term lesioned mice [$F_{(3,68)}=22.212$, ** $p < 0.01$ vs. Wt mice]. Episodic memory for "where" was significantly affected in 3-month-old transgenic mice; transgenic lesioned mice showed a slightly worse performance [$F_{(3,113)}=7.349$, ** $p < 0.01$ vs. Wt mice] (Fig. 2). Older mice (7 months of age) showed a more substantial deficit for the "where" paradigm when transgenic lesioned mice were compared to the other groups [$F_{(3,125)}=3.68$, * $p = 0.014$ vs. Wt Sham mice]. We also observed a worsening effect of the cholinergic lesion in APP/PS1 mice in long-term experiments [$F_{(3,66)}=6.23$, ** $p < 0.01$ vs. Wt mice]. Episodic memory ("when") was affected at 3 months of age in transgenic mice [$F_{(3,113)}=6.98$, ** $p < 0.01$ vs. Wt mice] (Fig. 2), but at 7 months of age only lesioned transgenic mice were significantly affected at this level [$F_{(3,122)}=37.056$, * $p < 0.01$ vs. other groups] (Fig. 2). Long-term studies showed a similar profile, i.e. there was increased impairment in transgenic mice with a cholinergic lesion [$F_{(3,64)}=17.801$, * $p < 0.01$ vs. Wt mice]. All 3 parameters analyzed were significantly impaired in 7-month-old lesioned transgenic mice, when A β deposition is well established. Altogether the NOD test showed that cholinergic lesions of the BFB significantly impaired episodic memory, particularly in older mice with higher amyloid burden.

Spatial learning and memory abilities were analyzed in all age groups using the Morris Water Maze test. We analyzed the time to locate the hidden platform during the acquisition phase and we used two-way ANOVA (group X day) to detect differences among groups. Further daily comparisons were performed with one-way ANOVA followed by Tukey-b test or Tamhane test, as required. We observed early cognitive impairment in 3-month-old acutely lesioned mice when we analyzed the time to locate the platform [$F_{(9,518)}=1.921$, $p=0.047$] (Fig. 3A). Daily analysis showed an overall delay to locate the platform for transgenic lesioned mice (day 1: [$F_{(3,144)}=9.79$, ** $p < 0.01$ vs. Wt Sham], day 2: [$F_{(3,140)}=17.910$, ** $p < 0.01$ vs. Wt Sham and Wt p-75 SAP, †† $p < 0.01$ vs. Wt Sham], day 3: [$F_{(3,133)}=17.346$, ** $p < 0.01$ vs. other groups, †† $p < 0.01$ vs. Wt Sham], day 4: [$F_{(3,134)}=14.025$, ** $p < 0.01$ vs. other groups]). In 7-month-old mice we observed cognitive alterations in animals bearing the APP/PS1 transgenes and we observed a worsening effect on those animals with acute cholinergic denervation (group X day) [$F_{(9,1008)}=2.781$, $p = 0.03$] (Fig. 3A). Further daily analysis corroborated these observations and we detected learning and memory impairment throughout the 4 days of the acquisition phase (day 1: [$F_{(3,272)}=10.611$, ** $p < 0.01$ vs. Wt Sham], day 2: [$F_{(3,272)}=22.398$, ** $p < 0.01$ vs. Wt Sham], day 3: [$F_{(3,262)}=13.605$, ** $p < 0.01$ vs. Wt Sham and APP/PS1 Sham, †† $p < 0.01$ vs. Wt Sham], day 4: [$F_{(3,266)}=24.109$, ** $p < 0.01$ vs. Wt Sham and APP/PS1 Sham, †† $p < 0.01$ vs. Wt Sham]). A similar profile was observed in 7-month-old mice with chronic cholinergic lesions. The presence of the APP/PS1 transgenes was enough to impair learning and memory abilities in the water maze; however, this effect was worsened in the presence of the cholinergic lesion (group X day) [$F_{(9,546)}=2.108$, $p = 0.027$] (Fig. 3A). Further daily analysis corroborated these observations (day 1: [$F_{(3,141)}=19.203$, ** $p < 0.01$ vs. Wt Sham]; day 2: [$F_{(3,151)}=9.385$, ** $p < 0.01$ vs. other groups, †† vs. Wt Sham]; day 3: [$F_{(3,143)}=19.199$, ** $p < 0.01$ vs. other groups, †† $p < 0.01$ vs. Wt Sham]; day 4: [$F_{(3,143)}=19.199$, ** $p < 0.01$ vs. other groups, †† $p < 0.01$ vs. Wt Sham]). We observed

some age-related learning and memory deficits in Wt mice that were not significantly different than those observed in Wt μ p75-SAP-treated mice.

We further analyzed the synergistic effect between the presence of a cholinergic lesion and the APP/PS1 transgenes along the fourth day of the acquisition phase, when differences among groups were most marked. At 3 months of age, we did not detect a significant transgene X lesion effect ($F_{(3,1)}=6.285$, $p = 0.651$); however, in older groups we detected a significant transgene X lesion effect, both in acute ($F_{(3,1)}=4.24$, * $p=0.04$) and long-term studies ($F_{(3,1)}=6.285$, * $p = 0.013$), supporting a synergistic effect between the APP/PS1 transgenes and the lesion with μ p75-SAP.

In the retention phase, which tests memory preservation, we measured the percentage of time spent by the animals in the quadrant number 2, where the platform was located during the acquisition phase (Fig. 3B). Using one-way ANOVA we did not detect statistical differences among 3-month-old groups of mice (μ p75-SAP transgenic vs. other groups) [$F_{(3,34)}=0.635$, $p = 0.597$]. Seven-month-old transgenic mice with acute or chronic cholinergic lesions showed difficulties in remembering the quadrant where the platform used to be located (quadrant 2) and they spent significantly shorter times in this area (acute lesion: [$F_{(3,62)}=2.858$, * $p = 0.04$ vs. other groups]; long-term lesion: [$F_{(3,34)}=3.134$, * $p = 0.038$ vs. other groups]). We observed that groups that presented some learning impairment during the acquisition phase also showed some limitations during the retention phase, although these differences did not reach statistical significance in the case of APP/PS1 Sham or Wt SAP-treated mice, when compared to Wt Sham mice (Fig. 3B). Altogether, our observations in the behavioral tests support the worsening effect of the cholinergic lesion in the pathological condition of APP/PS1 mice, affecting both episodic memory, as shown in the NOD test, as well as spatial and working memory in the Morris Water Maze test.

Effect of μ p75-SAP-induced Lesions on A β Deposition In Vivo and in Real Time

We used longitudinal in vivo MPM imaging to test the effect of μ p75-SAP-induced lesions on amyloid deposition in transgenic mice. Although we randomly assessed Wt mice, we did not detect any SPs in lesioned or Sham mice. Senile plaques in the cortex labeled with methoxy-XO4, were measured in transgenic mice and counted at 3 time points: immediately after the lesions; 7 days post-lesion; and 14 days post-lesion. Fluorescent angiograms were used as independent fiduciary markers to locate the same cortical regions at all 3 time points. We observed a significant increase in the deposition of SPs as soon as 7 days after the lesions when compared to Sham mice, both in young animals (~3 months of age) (Fig. 4A), with very limited amounts of A β , and in mice at ~7 months of age, with robust SP deposition (Fig. 4B). Although we observed a similar profile in SP deposition after cholinergic lesions, both in young and older mice, deposition rates were more robust in aged mice, supporting previous observations (8) and suggesting that cholinergic denervation triggers and accelerates amyloid deposition. This reinforcing effect of cholinergic denervation on amyloid deposition is depicted in Figure 4D–K. Sham-treated mice showed a rate of deposition of ~8 SPs/mm³/week, similar to that described previously (26). Long-term treated animals were assessed for in vivo deposition of A β at 3 months of age as well as one last time before death at 7 months of age. There was a significant increase in numbers of SPs deposited in mice with lesions when compared with Sham mice over this ~3.5 month period (Fig. 4).

We did not observe significant plaque clearance in any of the groups; therefore, the overall number of plaques increased over time. Vascular amyloid deposition in the APP/PS1 mouse is modest and we did not observe any gross changes in amyloid angiopathy progression or clearance due to the lesions.

Postmortem Assessment of A β deposition

Because the hippocampus cannot be chronically imaged in vivo using MPM, we assessed the effect of cholinergic denervation on hippocampal and cortical SP deposition by postmortem histochemical studies in APP/PS1 mice. Compared to Sham animals, mu p75-SAP-treated transgenic mice showed a significant increase in A β staining at different stages of aggregation (A β and compact SPs). This result was confirmed with both an anti-A β antibody and thioflavin S (TS) staining, which gave similar staining profiles (Fig. 5). Using the Student t-test for independent samples there was a significant increase in cortical plaque burden after denervation in all age groups studied, although this increase was more marked in 7-month-old mice, particularly in those with long-term lesions (Fig. 5A) (3 months acute: A β , * $p = 0.045$ vs. Sham; TS, * $p = 0.045$ vs. Sham, 7 months acute: A β , * $p = 0.018$ vs. Sham; TS, * $p = 0.026$ vs. Sham, 7 months long term: A β , * $p = 0.044$ vs. Sham; TS, * $p = 0.041$ vs. Sham).

We could not detect plaques in the hippocampus in 3-month-old Sham mice; only mu p75-SAP-injected mice had SPs at that early stage, indicating an acceleration of plaque deposition with a cholinergic lesion. There was a significant increase in amyloid burden in hippocampus of cholinergic denervated mice at 7 months of age (7 months acute: A β , * $p = 0.019$ vs. Sham; TS, * $p = 0.025$ vs. Sham, 7 months long term: A β , * $p = 0.022$ vs. Sham; TS, * $p = 0.046$ vs. Sham). Mean SP size was similar in all animals, both in the cortex (Fig. 5A) (3 months acute: A β , $p = 0.915$; TS, $p = 9.963$, 7 months acute: $p = 0.879$, 7 months long term: $p = 0.417$) and the hippocampus (7 months acute: A β , $p = 0.879$; TS, $p = 0.066$, 7 months long term: A β , $p = 0.158$; TS, $p = 0.950$), indicating that SP sizes are stable as the disease processes evolve.

We detected a significant increase in numbers of deposited plaques in 3-month-old acute lesioned mice in cortex (A β : * $p < 0.01$ vs. Sham, TS: * $p = 0.012$ vs. Sham). Similar profiles were observed in 7-month-old acute lesioned mice in cortex (Fig. 5A) (A β : * $p = 0.027$ vs. Sham, TS: * $p = 0.041$ vs. Sham) and hippocampus (A β : * $p = 0.032$ vs. Sham, TS: * $p = 0.038$ vs. Sham). A greater increase in numbers of SPs was observed in 7-month-old long-term denervated mice, both in cortex (A β : $p < 0.01$ vs. Sham, TS: * $p = 0.026$ vs. Sham) and hippocampus (A β : * $p = 0.044$ vs. Sham, TS: * $p = 0.042$ vs. Sham), suggesting that increased burden is due to an increase on the number of newly deposited SPs. Thus, our data indicate that cholinergic lesions can rapidly increase A β deposition in denervated areas, cortex and hippocampus, but also maintain a long-term synergistic effect on A β deposition.

Effect of Cholinergic Lesions on tau Phosphorylation

We analyzed the effect of cholinergic denervation with mu p75-SAP in tau phosphorylation in the cortex of Wt and transgenic mice and observed an increase in tau phosphorylation in Wt denervated mice as a consequence of administering the immunotoxin mu p75-SAP (Fig. 6). However, these values were significantly lower than those observed in transgenic mice, suggesting that the effect might be related to the increase in A β deposition and not just to the administration of the toxin. One-way ANOVA followed by Tukey-b or Tamhane tests showed a ~4-fold increase on tau phosphorylation in all age groups of denervated transgenic mice, including 3 months acute mice [$F_{(3,28)}=16.455$, * $p < 0.01$ vs. other groups] (Fig. 6A), 7 months acute mice [$F_{(3,19)}=8.896$, * $p = 0.01$ vs. other groups, † $p = 0.001$ vs. Wt Sham] (Fig. 6B) and 7 months long-term mice [$F_{(3,28)}=6.720$, * $p=0.001$ vs. other groups, † $p=0.001$ vs. Wt Sham] (Fig. 6C).

DISCUSSION

Amyloid deposition, abnormal tau phosphorylation and neurofibrillary tangle formation and neuronal loss are the major hallmarks of AD but current animal models do not recapitulate all of these neuropathological features. In particular, the selective early loss of cholinergic neurons has not been modelled in the context of AD pathology. Although loss of BFB cholinergic neurons may not be the initial neurodegenerative event in AD (7), these neurons seem to be particularly vulnerable in AD. Presynaptic cholinergic markers are dramatically reduced and there is marked neuronal loss in the nucleus basalis of Meynert of AD patients (6, 27, 28). It has been previously suggested that the dual implication of choline as a precursor for both acetylcholine and membrane phosphatidylcholine might be responsible for this special vulnerability of cholinergic neurons (6, 29). On the other hand, A β , in different states of aggregation, continues to be the main target in the development of new therapeutic approaches although the ultimate neurotoxic mechanisms implied in the onset of the disease are not completely understood. To establish a direct relationship between both AD hallmarks, we hypothesized that BFB cholinergic denervation may induce or accelerate A β deposition.

APP/PS1 mice show early A β deposition, i.e. by the age of 4 months. As in other AD transgenic mice, however, no neuronal loss is spontaneously observed in these animals (11). Administering mu p75-SAP to APP/PS1 mice allows the study of a more complex version of the illness, including specific cholinergic denervation. With this paradigm, we observed cholinergic denervation within 7 days of injecting the toxin that reached ~40% to 50% of AChE activity in the cortex and hippocampus, without affecting non-innervated areas, such as the striatum. We confirmed that mu p75-SAP selectively targets cholinergic neurons bearing the receptor p75^{NTR} without affecting parvalbumin-positive neurons (7, 14). Moreover, our behavioral data show no locomotor activity alterations in immunotoxin-treated animals, thereby supporting the likelihood that other distant neurons, such as Purkinje cells bearing the p75^{NTR} receptor, are preserved. We cannot rule out the possibility that p75^{NTR}-positive progenitor cells in the subventricular zone or dentate gyrus (30, 31) could be affected after the lesions; therefore, cell proliferation and neurogenesis could be altered. However, such effects would not be expected to cause the dramatic effects on memory and A β deposition that we observed.

The NOD behavioral test showed that APP/PS1 mice have episodic memory deficits as early as 3 months of age, supporting the sensitivity of this test. This parallels observations in AD patients who show early alterations of episodic memory (32). At older stages, we observed that both APP/PS1 and Wt mice have decreased abilities in the NOD test and that this effect was worsened in the presence of cholinergic lesions. Our observations were confirmed in the Morris Water Maze test for working and spatial memory, i.e. young lesioned APP/PS1 mice were only mildly impaired in the acquisition phase, whereas older APP/PS1 lesioned mice showed significantly worse patterns vs. Wt or Sham-lesioned transgenic mice. Moreover, this effect was worsened in long-term lesioned mice, i.e. those bearing a higher amyloid burden. We observed a synergistic effect to worsen learning and memory abilities in animals both with a cholinergic lesion and bearing the APP/PS1 transgenes, implying that cholinergic neuron loss exacerbates age-related A β -induced memory deficits.

We assessed amyloid deposition in vivo using MPM. This approach allowed us to follow the appearance of new SPs over time by re-imaging the same cortical areas for up to 3.5 months after the cholinergic lesions. In our hands, specific BFB denervation accelerated SP deposition in APP/PS1 mice. Previous studies have shown that 7-month-old APP/PS1 mice deposit SPs at a similar rate to that measured here (4, 8, 26). Although at slower rates than adults, young (~3 months old) APP/PS1 mice deposit more SPs after removing cholinergic

innervation to the cortex than Sham operated mice. This indicates that it is not the actual physical lesion that leads to amyloid deposition but the specific cholinergic denervation. Similarly, adult APP/PS1 mice (~7 months of age) treated with mu p75-SAP showed higher amyloid burden as soon as 1 week after the lesion. Moreover, although high variability was observed, our results showed a tendency of long-term lesioned mice to maintain increased deposition rates during the 3 months following the lesion, suggesting that the effect of cholinergic denervation on A β deposition is long-lasting once the lesion is completely established.

Although extremely powerful, our MPM does not allow us to assess other relevant brain regions such as the hippocampus. Nevertheless, our *in vivo* observations that removal of cholinergic innervation can induce and accelerate SP deposition were confirmed by postmortem A β immunohistochemistry both in the cortex and hippocampus. We observed that plaque size was not affected, implying that SPs are quite stable once deposited, as previously described (4, 33). In fact, increased SP burden was due to a rise in SP number. Previous studies in AD mice have shown that more nonspecific lesioning of the perforant cortical pathways reduces APP-immunoreactivity and A β burden in denervated dentate gyrus (34, 35), whereas other studies also show no effect on APP or SP deposition in the hippocampus after fimbria-fornix transection (36). On the other hand, in other animal models, more specific BFB cholinergic lesions have shown some capacity to increase APP levels in the cortex and hippocampus (37, 38), as well as increasing A β deposition as amyloid angiopathy (39). In our hands, selective and specific cholinergic denervation leads to increased SP deposition, and this effect seems to be more prominent in the cortex.

Although we were not able to detect neurofibrillary tangles using immunohistochemistry, Western blot analysis revealed tau phosphorylation in the cortex of APP/PS1 mice, as previously described (40); this was increased in denervated APP/PS1 mice. This finding also underscores the relevance of our animal model as a paradigm for AD.

The underlying explanation for the selective vulnerability of different brain regions in AD remains unclear. Previous studies in the locus coeruleus suggest that specific groups of neurons under situations of stress may increase amyloid generation and favor A β oligomerization (41). Moreover, when locus coeruleus cortical noradrenergic innervation is removed in AD mice, augmented amyloid plaque deposits and behavioral impairments are observed (42). A similar situation may occur in the cholinergic system. In our model, cholinergic innervation is removed to relevant areas in learning and memory that are specifically affected in AD. We are aware of previous studies in which increased synaptic transmission results in increased A β production (43); however, reduced synaptic activity also causes detrimental effects on synapses and memory, despite reducing plaques (44). We cannot exclude the possibility that remaining cholinergic neurons from the BFB, or even intracortical cholinergic neurons, might to some extent compensate for the insult, resulting in an overall increase in synaptic transmission. Although it has been reported that precuneus ChAT activity is reduced only when AD is completely established (45), other recent studies have shown that cholinergic degeneration and dysfunction in AD begin before the onset of dementia, in parallel with SP deposition (46). In this sense, treatment with muscarinic receptor 1 agonists can reduce A β in AD patients, suggesting this approach as a potential amyloid lowering therapy of AD (47, 48). Although to our knowledge the direct implication of the cholinergic system in A β release or seeding has not been clarified, it has been shown that A β released at the synapse may serve as seed for SP deposition. Seeds seem to migrate along defined neuronal pathways to non-contiguous but axonally interconnected regions (49, 50). Altogether, our data suggest that cholinergic denervation may contribute to the deposition of A β and synergistically contribute to learning and memory impairment, as

observed in AD. This could also open the door to treatments that may target specific regions (51), and that could ultimately provide a simpler therapeutic approach.

Acknowledgments

We would like to thank Mrs. Raquel Rey-Brea for her excellent technical assistance.

Disclosure of Funding: RYC-2008-02333, ISCIII-Subdirección General de Evaluación y Fomento de la Investigación (PS09/00969), Junta de Andalucía, Proyectos de Excelencia (P11-CTS-7847), Fundación Dr. Eugenio Rodríguez Pascual 2012 (MG-A); NIH R01 EB000768 (BJB); NIH R00 AG033670 (TLS).

REFERENCES

- Gomez-Isla T, Hollister R, West H, et al. Neuronal loss correlates with but exceeds neurofibrillary tangles in Alzheimer's disease. *Ann Neurol.* 1997; 41:17–24. [PubMed: 9005861]
- Walsh DM, Selkoe DJ. Deciphering the molecular basis of memory failure in Alzheimer's disease. *Neuron.* 2004; 44:181–193. [PubMed: 15450169]
- Roberson MR, Harrell LE. Cholinergic activity and amyloid precursor protein metabolism. *Brain Res Brain Res Rev.* 1997; 25:50–69. [PubMed: 9370050]
- Meyer-Luehmann M, Spires-Jones TL, Prada C, et al. Rapid appearance and local toxicity of amyloid-beta plaques in a mouse model of Alzheimer's disease. *Nature.* 2008; 451:720–724. [PubMed: 18256671]
- Brendza RP, Bacsikai BJ, Cirrito JR, et al. Anti-Abeta antibody treatment promotes the rapid recovery of amyloid-associated neuritic dystrophy in PDAPP transgenic mice. *J Clin Invest.* 2005; 115:428–433. [PubMed: 15668737]
- Rossner S, Ueberham U, Schliebs R, et al. The regulation of amyloid precursor protein metabolism by cholinergic mechanisms and neurotrophin receptor signaling. *Prog Neurobiol.* 1998; 56:541–569. [PubMed: 9775403]
- Berger-Sweeney J, Stearns NA, Murg SL, et al. Selective immunolesions of cholinergic neurons in mice: effects on neuroanatomy, neurochemistry, and behavior. *J Neurosci.* 2001; 21:8164–8173. [PubMed: 11588189]
- Garcia-Alloza M, Robbins EM, Zhang-Nunes SX, et al. Characterization of amyloid deposition in the APP^{swe}/PS1^{ΔE9} mouse model of Alzheimer disease. *Neurobiol Dis.* 2006; 24:516–524. [PubMed: 17029828]
- Jankowsky JL, Fadale DJ, Anderson J, et al. Mutant presenilins specifically elevate the levels of the 42 residue beta-amyloid peptide in vivo: evidence for augmentation of a 42-specific gamma secretase. *Hum Mol Genet.* 2004; 13:159–170. [PubMed: 14645205]
- Jankowsky JL, Melnikova T, Fadale DJ, et al. Environmental enrichment mitigates cognitive deficits in a mouse model of Alzheimer's disease. *J Neurosci.* 2005; 25:5217–5224. [PubMed: 15917461]
- Perez SE, Dar S, Ikonovic MD, et al. Cholinergic forebrain degeneration in the APP^{swe}/PS1^{ΔE9} transgenic mouse. *Neurobiol Dis.* 2007; 28:3–15. [PubMed: 17662610]
- German DC, Yazdani U, Speciale SG, et al. Cholinergic neuropathology in a mouse model of Alzheimer's disease. *J Comp Neurol.* 2003; 462:371–381. [PubMed: 12811807]
- Hunter CL, Quintero EM, Gilstrap L, Bhat NR, et al. Minocycline protects basal forebrain cholinergic neurons from mu p75-saporin immunotoxic lesioning. *Eur J Neurosci.* 2004; 19:3305–3316. [PubMed: 15217386]
- Moreau PH, Cosquer B, Jeltsch H, et al. Neuroanatomical and behavioral effects of a novel version of the cholinergic immunotoxin mu p75-saporin in mice. *Hippocampus.* 2008; 18:610–622. [PubMed: 18306300]
- Dere E, Huston JP, De Souza Silva MA. Integrated memory for objects, places, and temporal order: evidence for episodic-like memory in mice. *Neurobiol Learn Mem.* 2005; 84:214–221. [PubMed: 16102980]

16. Garcia-Alloza M, Zaldúa N, Diez-Ariza M, et al. Effect of selective cholinergic denervation on the serotonergic system: implications for learning and memory. *J Neuropathol Exp Neurol.* 2006; 65:1074–1081. [PubMed: 17086104]
17. Nag N, Baxter MG, Berger-Sweeney JE. Efficacy of a murine-p75-saporin immunotoxin for selective lesions of basal forebrain cholinergic neurons in mice. *Neurosci Lett.* 2009; 452:247–251. [PubMed: 19150485]
18. Berger-Sweeney J, Heckers S, Mesulam MM, et al. Differential effects on spatial navigation of immunotoxin-induced cholinergic lesions of the medial septal area and nucleus basalis magnocellularis. *J Neurosci.* 1994; 14:4507–4519. [PubMed: 8027790]
19. Morris R. Developments of a water-maze procedure for studying spatial learning in the rat. *J Neurosci Methods.* 1984; 11:47–60. [PubMed: 6471907]
20. Skoch A, Jirak D, Vyhnánovská P, et al. Classification of calf muscle MR images by texture analysis. *MAGMA.* 2004; 16:259–267. [PubMed: 15045590]
21. Klunk WE, Bacskai BJ, Mathis CA, et al. Imaging Abeta plaques in living transgenic mice with multiphoton microscopy and methoxy-X04, a systemically administered Congo red derivative. *J Neuropathol Exp Neurol.* 2002; 61:797–805. [PubMed: 12230326]
22. Garcia-Alloza M, Gregory J, Kuchibhotla KV, et al. Cerebrovascular lesions induce transient beta-amyloid deposition. *Brain.* 2011; 134:3697–3707. [PubMed: 22120142]
23. Garcia-Alloza M, Borrelli LA, Hyman BT, et al. Antioxidants have a rapid and long-lasting effect on neuritic abnormalities in APP:PS1 mice. *Neurobiol Aging.* 2010; 31:2058–2068. [PubMed: 19124175]
24. Wang XD, Chen XQ, Yang HH, et al. Comparison of the effects of cholinesterase inhibitors on [3H]MK-801 binding in rat cerebral cortex. *Neurosci Lett.* 1999; 272:21–24. [PubMed: 10507533]
25. Wiesehan K, Buder K, Linke RP, et al. Selection of D-amino-acid peptides that bind to Alzheimer's disease amyloid peptide abeta1-42 by mirror image phage display. *Chembiochem.* 2003; 4:748–753. [PubMed: 12898626]
26. Garcia-Alloza M, Borrelli LA, Rozkalne A, et al. Curcumin labels amyloid pathology in vivo, disrupts existing plaques, and partially restores distorted neurites in an Alzheimer mouse model. *J Neurochem.* 2007; 102:1095–1104. [PubMed: 17472706]
27. Chozick B. The nucleus basalis of Meynert in neurological dementing disease: a review. *Int J Neurosci.* 1987; 37:31–48. [PubMed: 2960633]
28. Vana L, Kanaan NM, Ugwu IC, et al. Progression of tau pathology in cholinergic Basal forebrain neurons in mild cognitive impairment and Alzheimer's disease. *Am J Pathol.* 2011; 179:2533–2550. [PubMed: 21945902]
29. Wurtman RJ. Choline metabolism as a basis for the selective vulnerability of cholinergic neurons. *Trends Neurosci.* 1992; 15:117–122. [PubMed: 1374967]
30. Bernabeu RO, Longo FM. The p75 neurotrophin receptor is expressed by adult mouse dentate progenitor cells and regulates neuronal and non-neuronal cell genesis. *BMC Neurosci.* 2010; 11:136. [PubMed: 20961458]
31. Sothibundhu A, Li QX, Thangnipon W, et al. Abeta(1-42) stimulates adult SVZ neurogenesis through the p75 neurotrophin receptor. *Neurobiol Aging.* 2009; 30:1975–1985. [PubMed: 18374455]
32. Pozueta A, Rodriguez-Rodriguez E, Vazquez-Higuera JL, et al. Detection of early Alzheimer's disease in MCI patients by the combination of MMSE and an episodic memory test. *BMC Neurol.* 2011; 11:78. [PubMed: 21702929]
33. Christie RH, Bacskai BJ, Zipfel WR, et al. Growth arrest of individual senile plaques in a model of Alzheimer's disease observed by in vivo multiphoton microscopy. *J Neurosci.* 2001; 21:858–864. [PubMed: 11157072]
34. Sheng JG, Price DL, Koliatsos VE. Disruption of corticocortical connections ameliorates amyloid burden in terminal fields in a transgenic model of Abeta amyloidosis. *J Neurosci.* 2002; 22:9794–9799. [PubMed: 12427835]
35. Lazarov O, Lee M, Peterson DA, et al. Evidence that synaptically released beta-amyloid accumulates as extracellular deposits in the hippocampus of transgenic mice. *J Neurosci.* 2002; 22:9785–9793. [PubMed: 12427834]

36. Liu L, Ikonen S, Tapiola T, et al. Fimbria-fornix lesion does not affect APP levels and amyloid deposition in the hippocampus of APP+PS1 double transgenic mice. *Exp Neurol*. 2002; 177:565–574. [PubMed: 12429202]
37. Lin L, LeBlanc CJ, Deacon TW, et al. Chronic cognitive deficits and amyloid precursor protein elevation after selective immunotoxin lesions of the basal forebrain cholinergic system. *Neuroreport*. 1998; 9:547–552. [PubMed: 9512404]
38. Leanza G. Chronic elevation of amyloid precursor protein expression in the neocortex and hippocampus of rats with selective cholinergic lesions. *Neurosci Lett*. 1998; 257:53–56. [PubMed: 9857964]
39. Roher AE, Kuo YM, Potter PE, et al. Cortical cholinergic denervation elicits vascular A beta deposition. *Ann N Y Acad Sci*. 2000; 903:366–373. [PubMed: 10818527]
40. Shi JQ, Shen W, Chen J, et al. Anti-TNF-alpha reduces amyloid plaques and tau phosphorylation and induces CD11c-positive dendritic-like cell in the APP/PS1 transgenic mouse brains. *Brain Res*. 2011; 1368:239–247. [PubMed: 20971085]
41. Muresan, V.; Muresan, Z. Society for Neuroscience Meeting, Washington DC: Online; 2011. Locus coeruleus neurons are highly vulnerable to stress, and initiate Alzheimer's disease pathology in remote regions of the brain. Program number 12.01
42. Heneka MT, Ramanathan M, Jacobs AH, et al. Locus ceruleus degeneration promotes Alzheimer pathogenesis in amyloid precursor protein 23 transgenic mice. *J Neurosci*. 2006; 26:1343–1354. [PubMed: 16452658]
43. Cirrito JR, Kang JE, Lee J, et al. Endocytosis is required for synaptic activity-dependent release of amyloid-beta in vivo. *Neuron*. 2008; 58:42–51. [PubMed: 18400162]
44. Tampellini D, Capetillo-Zarate E, Dumont M, et al. Effects of synaptic modulation on beta-amyloid, synaptophysin, and memory performance in Alzheimer's disease transgenic mice. *J Neurosci*. 2010; 30:14299–14304. [PubMed: 20980585]
45. Ikonomic MD, Klunk WE, Abrahamson EE, et al. Precuneus amyloid burden is associated with reduced cholinergic activity in Alzheimer disease. *Neurology*. 2011; 77:39–47. [PubMed: 21700583]
46. Potter PE, Rauschkolb PK, Pandya Y, et al. Pre- and post-synaptic cortical cholinergic deficits are proportional to amyloid plaque presence and density at preclinical stages of Alzheimer's disease. *Acta Neuropathol*. 2011; 122:49–60. [PubMed: 21533854]
47. Hock C, Konietzko U, Streffer JR, et al. Antibodies against beta-amyloid slow cognitive decline in Alzheimer's disease. *Neuron*. 2003; 38:547–554. [PubMed: 12765607]
48. Nitsch RM, Deng M, Tennis M, et al. The selective muscarinic M1 agonist AF102B decreases levels of total A beta in cerebrospinal fluid of patients with Alzheimer's disease. *Ann Neurol*. 2000; 48:913–918. [PubMed: 11117548]
49. Eisele YS, Bolmont T, Heikenwalder M, et al. Induction of cerebral beta-amyloidosis: intracerebral versus systemic A beta inoculation. *Proc Natl Acad Sci U S A*. 2009; 106:12926–12931. [PubMed: 19622727]
50. Jucker M, Walker LC. Pathogenic protein seeding in Alzheimer disease and other neurodegenerative disorders. *Ann Neurol*. 2011; 70:532–540. [PubMed: 22028219]
51. Harris JA, Devidze N, Verret L, et al. Transsynaptic progression of amyloid-beta-induced neuronal dysfunction within the entorhinal-hippocampal network. *Neuron*. 2010; 68:428–441. [PubMed: 21040845]

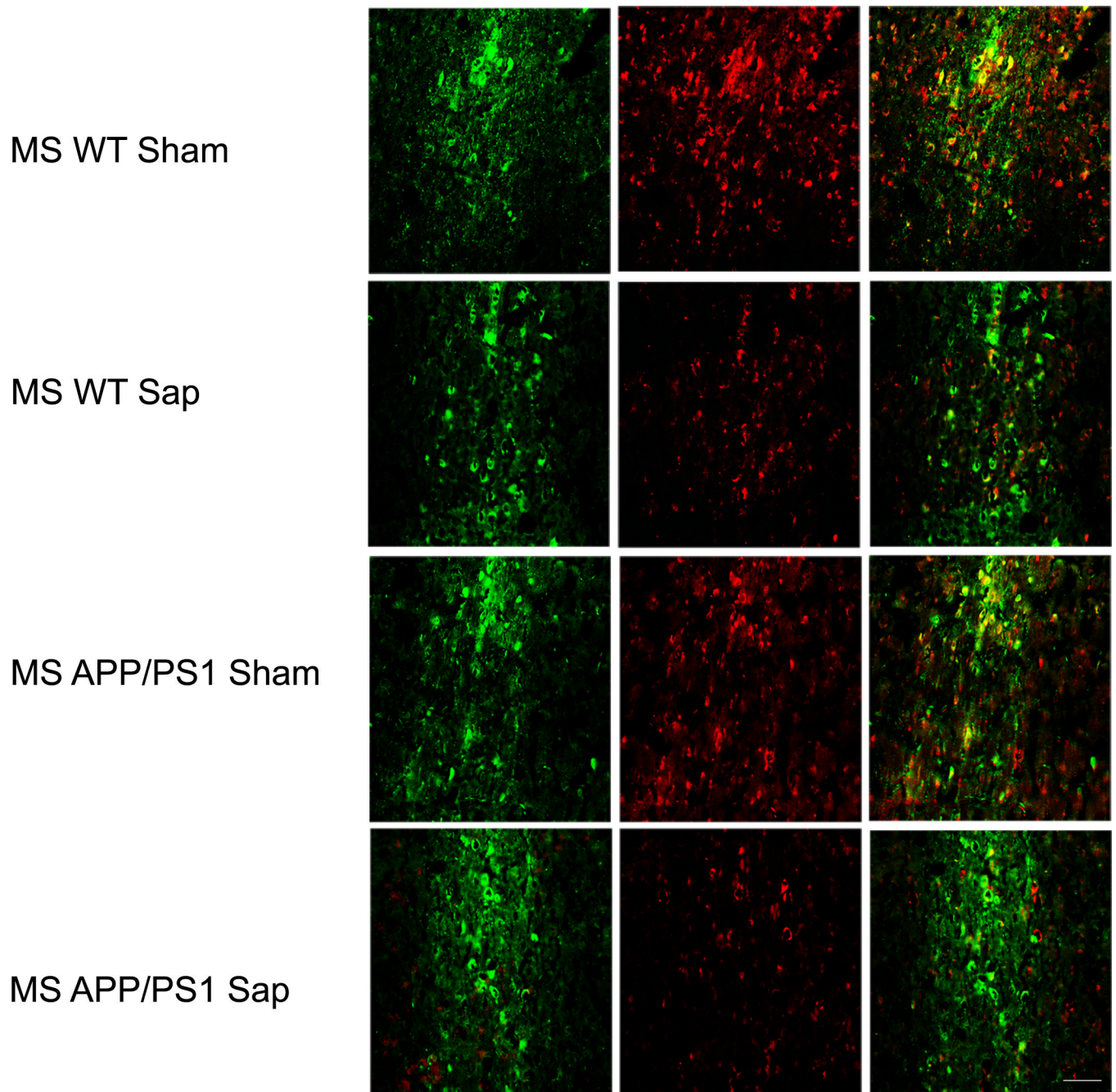


Figure 1. Cholinergic denervation after murine p75^{NTR} saporin (Sap) lesions of the basal forebrain in wild type (WT) and APP/PS1 mice. There is reduction of choline acetyltransferase immunostaining (red) in the medial septum at 2 weeks after the lesion compared to vehicle-treated (Sham) mice; γ -aminobutyric acid-releasing (GABAergic) neurons indicated by parvalbumin immunostaining (green) appear preserved. Scale bar = 250 μ m.

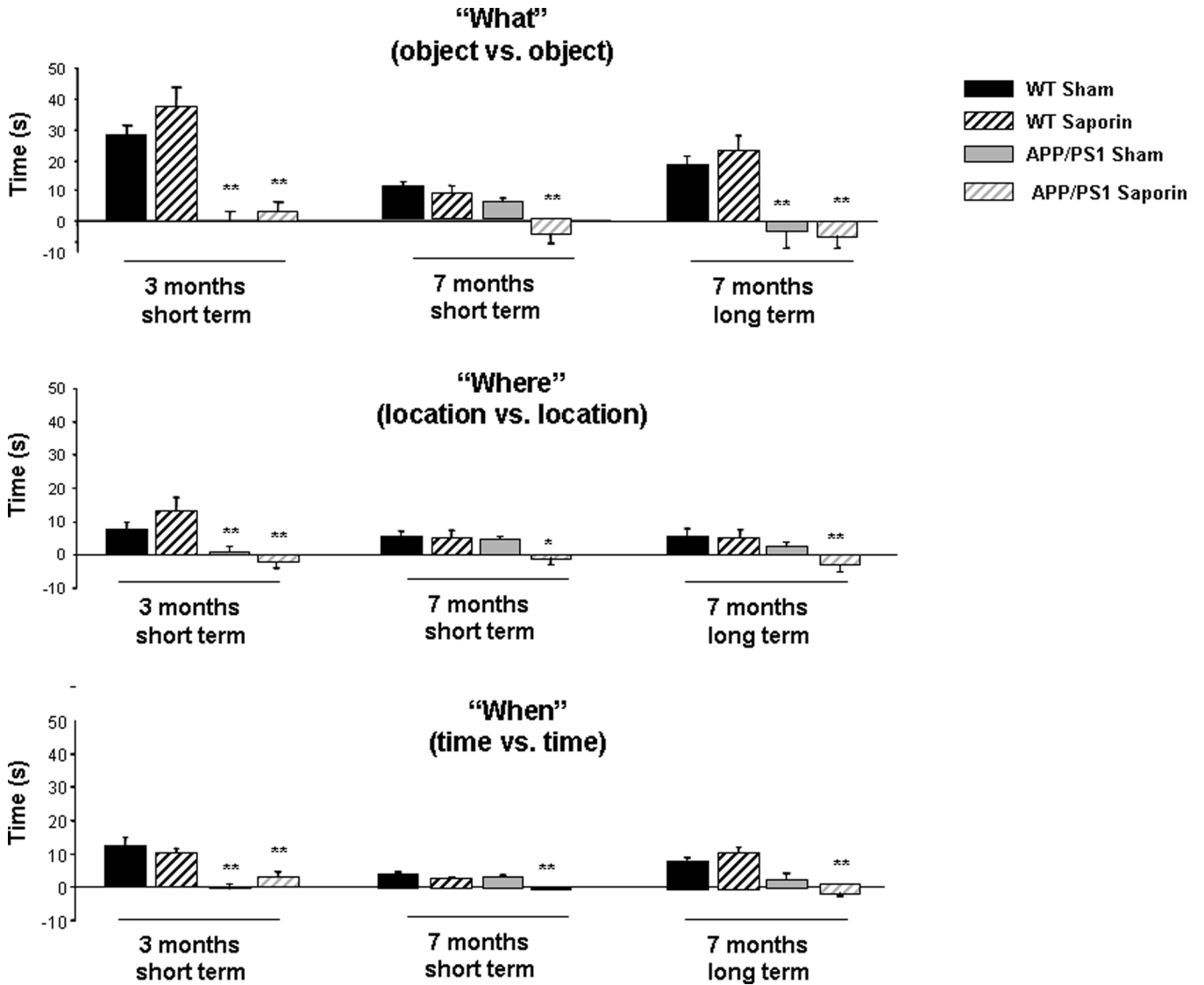
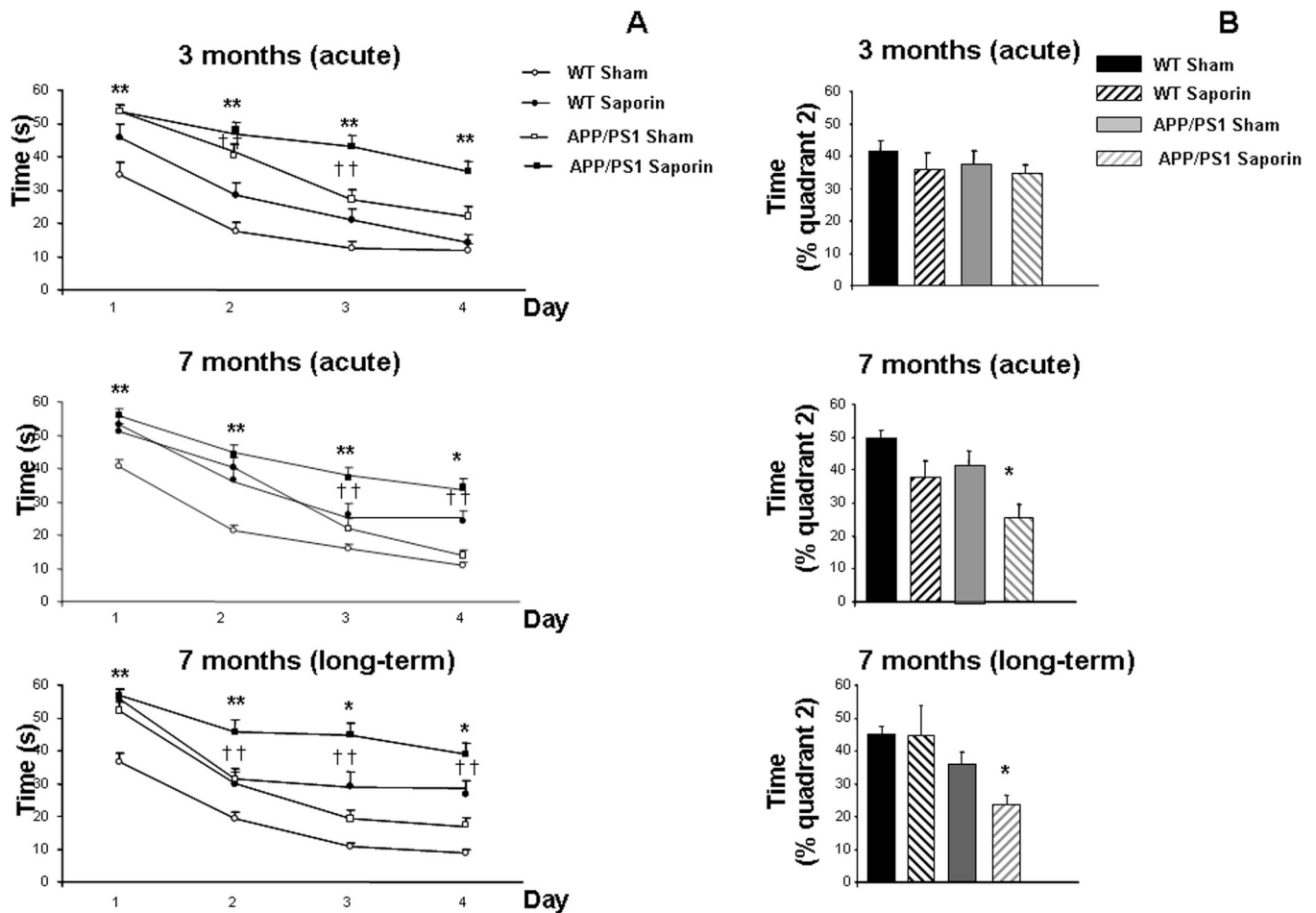


Figure 2. Effect of basal forebrain cholinergic denervation (Saporin) in APP/PS1 mice on episodic memory evaluated with the new object discrimination (NOD) test. There was an overall worsening performance with age for all paradigms under study (age X transgene effect: what: $[F_{(2,1)}=12.243, ** p < 0.01]$, where: $[F_{(2,1)}=13.81, * p = 0.023]$, when: $[F_{(2,1)}=19.710, ** p < 0.01]$). There was significant impairment in 3-month-old (short term) lesioned mice for "what", "where" and "when" parameters ($* p < 0.05$ vs. Wt [WT] Sham [vehicle-treated] and WT Saporin). There was a worsening effect of cholinergic denervation in older APP/PS1 lesioned mice (7 months old) ($* p < 0.05$ vs. the other groups). One-way ANOVA for independent samples followed by Tukey-b or Tamahane test as needed.

**Figure 3.**

Effect of cholinergic denervation (Saporin) in APP/PS1 mice on spatial learning and memory evaluated using the Morris water maze test. Data are representative of 7 to 14 mice. (A) Young mice (3 months old) had some impairment locating the hidden platform during the 4 days of the acquisition phase; this effect was worsened in older transgenic mice (7 months), with acute and long-term cholinergic lesions. Differences were detected by two-way ANOVA (group X day) * $p < 0.05$. y-axis = time to locate the hidden platform. Daily analysis showed an overall delay to locate the platform for 3-month-old transgenic lesioned mice (day 1: [$F_{(3,144)}=9.79$, ** $p < 0.01$ vs. wild-type (WT) Sham], day 2: [$F_{(3,140)}=17.910$, ** $p < 0.01$ vs. WT Sham and WT p-75 SAP, †† $p < 0.01$ vs. WT Sham], day 3: [$F_{(3,133)}=17.346$, ** $p < 0.01$ vs. other groups, †† $p < 0.01$ vs. WT Sham], day 4: [$F_{(3,134)}=14.025$, ** $p < 0.01$ vs. other groups]). In 7-month-old mice we observed cognitive alterations in animals bearing the APP/PS1 transgenes and we observed a worsening effect on those animals with acute cholinergic denervation (day 1: [$F_{(3,272)}=10.611$, ** $p < 0.01$ vs. WT Sham], day 2: [$F_{(3,272)}=22.398$, ** $p < 0.01$ vs. WT Sham], day 3: [$F_{(3,262)}=13.605$, ** $p < 0.01$ vs. WT Sham and APP/PS1 Sham, †† $p < 0.01$ vs. WT Sham], day 4: [$F_{(3,266)}=24.109$, ** $p < 0.01$ vs. WT Sham and APP/PS1 Sham, †† $p < 0.01$ vs. WT Sham]). A similar profile was observed in 7-month-old mice with chronic cholinergic lesions. The presence of the APP/PS1 transgenes was enough to impair learning and memory abilities in the water maze, however this effect was worsened in the presence of the cholinergic lesion (day 1: [$F_{(3,141)}=19.203$, ** $p < 0.01$ vs. WT Sham], day 2: [$F_{(3,151)}=9.385$, ** $p < 0.01$ vs. other groups, †† vs. WT Sham], day 3: [$F_{(3,143)}=19.199$, ** $p < 0.01$ vs. other groups, †† vs. WT Sham], day 4: [$F_{(3,143)}=19.199$, ** $p < 0.01$ vs. other groups, †† vs. WT Sham]).

< 0.01 vs. other groups, †† $p < 0.01$ vs. WT Sham], day 4: [$F_{(3,143)}=19.199$, ** $p < 0.01$ vs. other groups, †† $p < 0.01$ vs. WT Sham]). **(B)** During the retention phase there was significant memory impairment in 7-month-old transgenic lesioned mice with acute and long-term cholinergic lesions. Differences were detected using one-way ANOVA followed by Tukey-b test.

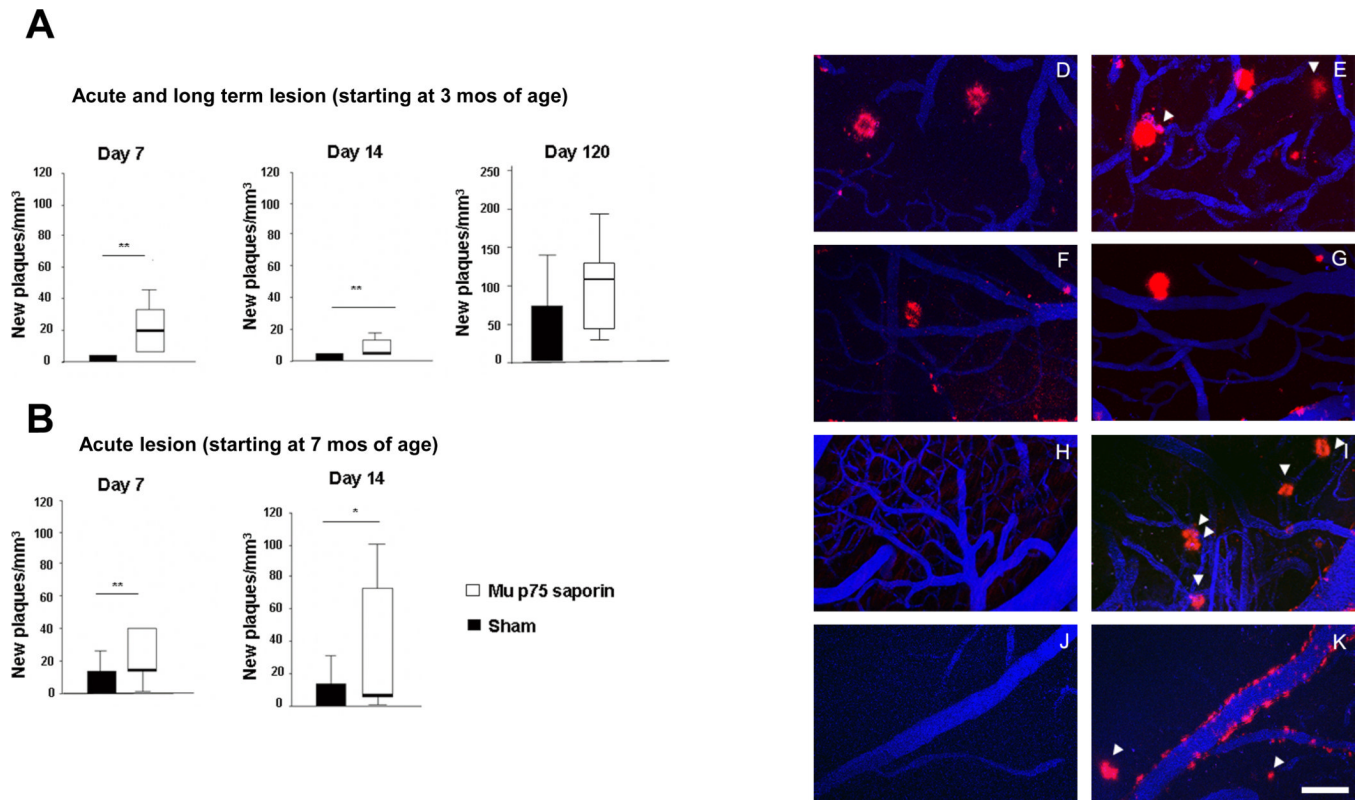
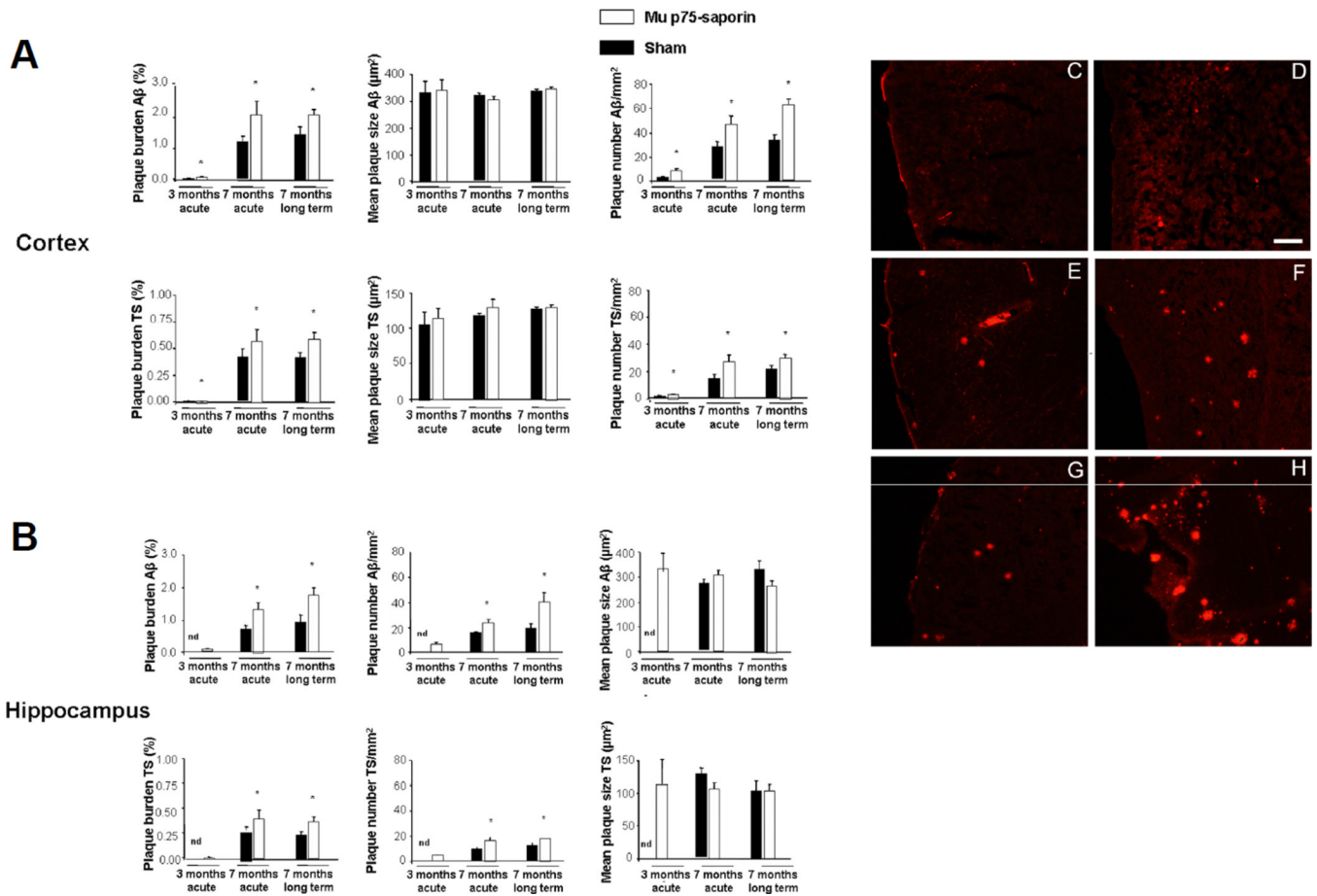


Figure 4.

Increased numbers of new senile plaques (SPs) in the cortex of APP/PS1 mice with and without murine p75^{NTR} saporin (mu p75-SAP) lesions were detected using *in vivo* multiphoton microscopy. Medians, maximums and minimums are shown and statistical differences were detected between both groups using Mann-Whitney U test for independent samples. **(A)** Numbers of plaques appearing per mm³ in ~3-month-old APPswe/PS1dE9 mice 7 and 14 days after the lesions (7 days: ** $p = 0.006$ vs. Sham; 14 days: ** $p < 0.01$ vs. Sham). When animals were compared between the day of the lesion and 120 days later there was an increase in SPs in lesioned animals, although differences did not reach statistical significance ($p = 0.190$ vs. Sham mice). **(B)** The same profile was observed in ~7-month-old mice (7 days: ** $p < 0.01$ vs. Sham; 14 days: * $p = 0.044$ vs. Sham). **(D–K)** Examples of SP deposition in an APPswe/PS1dE9 mouse 7 days after mu p75-SAP lesion (**D**, day 0; **E**, day 7) vs. a Sham mouse (**F**, day 0; **G**, day 7). Higher deposition was observed in lesioned APPswe/PS1dE9 mice 120 days after surgery (**H**, day 0; **I**, day 120), vs. a Sham mouse (**J**, day 0; **K**, day 120). The same fields were located using Texas Red dextran 70K (blue) for the angiograms and amyloid deposits were stained with methoxy-XO4 (red). White arrows indicate new amyloid deposits. Scale bar = 85 μm.

**Figure 5.**

Postmortem assessment of senile plaque (SP) deposition with anti- β -amyloid ($A\beta$) antibody and thioflavin S (TS) staining in cortex and hippocampus of APP/PS1 mice with or without murine p75^{NTR} saporin (mu p75-SAP)-induced lesions. (**A**, **B**) There was a significant increase in plaque burden in all lesioned mice, although this effect was greater in 7-month-old mice, particularly in those with long-term lesions. The increase in amyloid burden, both in cortex (**A**) and hippocampus (**B**) was not due to increased plaque size but to an increase in the number of new deposited SPs. Data are representative of 3 to 6 mice per group. Statistical differences were detected by Student t-test for independent samples and Mann-Whitney U-test for independent samples in the case of number of plaques per mm². * $p < 0.05$. (**C–H**) Examples of $A\beta$ immunostaining in the cortex: **C**, Sham 3 months acute; **D**, Mu p75-SAP, 3 months acute; **E**, Sham 7 months acute; **F**, Mu p75-SAP, 7 months acute; **G**, Sham 7 months long-term; **H**, Mu p75-SAP 7 months long-term. Scale bar = 250 μ m.

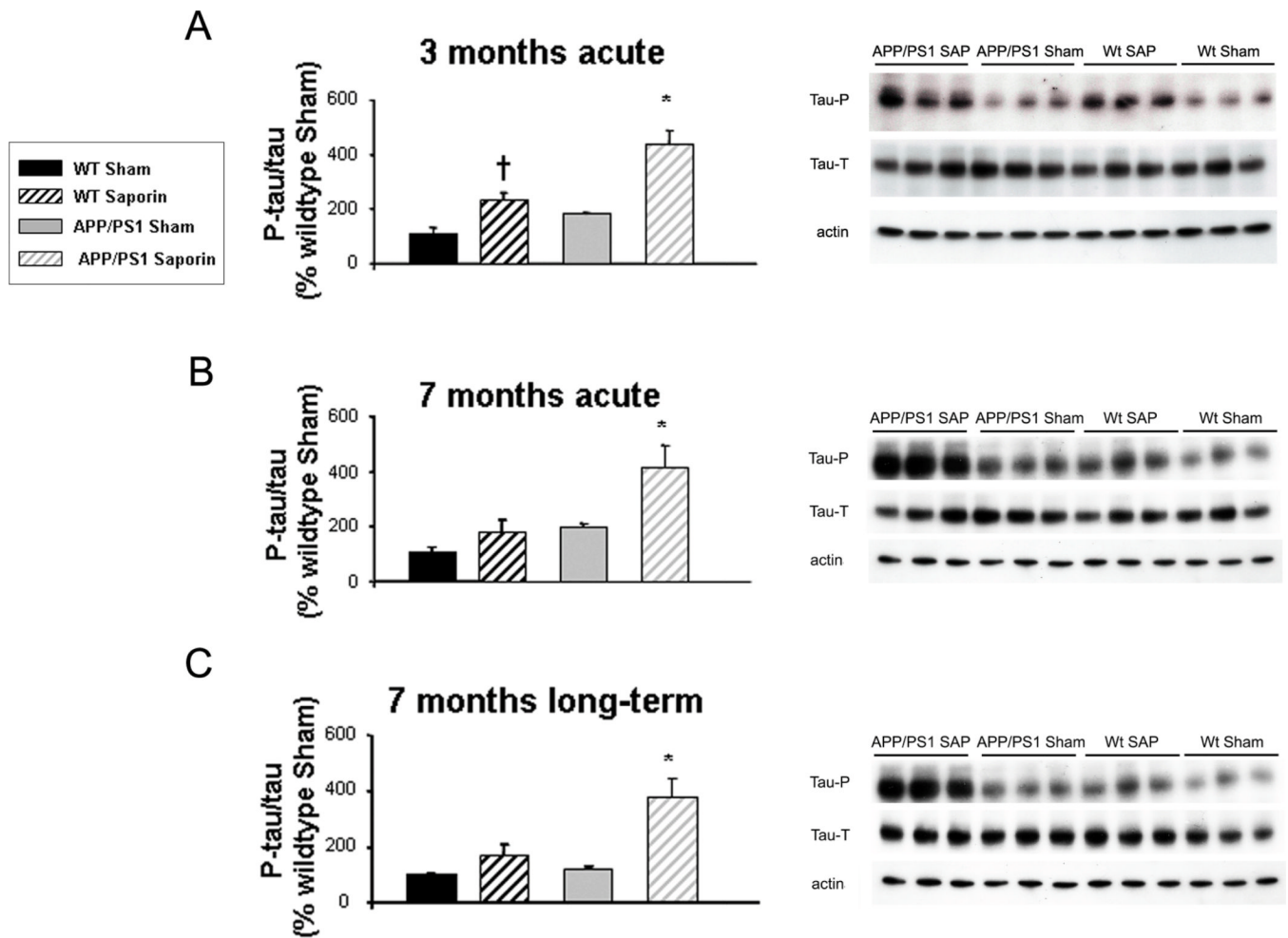


Figure 6. Increased tau phosphorylation in transgenic mice acutely lesioned with murine p75^{NTR} saporin (SAP) at 3 months and 7 months of age and in long-term lesioned 7-month-old mice. Phosphorylated tau/ total tau ratios (left panels) are expressed as percentage of wild-type (WT) vehicle-treated (Sham) values. Differences were detected by one-way ANOVA followed by Tukey-b test or Tamhane test as required (* $p < 0.05$). **(A)** In 3-month acute lesions, $F_{(3,28)} = 16.455$, (* $p < 0.01$ vs. other groups, † $p = 0.001$ vs. WT Sham). **(B)** 7-month acute lesions $F_{(3,19)} = 8.896$, (* $p = 0.01$ vs. other groups). **(C)** 7-month long-term lesions, $F_{(3,28)} = 6.720$, (* $p = 0.001$ vs. other groups). Right panels: Examples of western blot for total tau, phospho-tau and α -tubulin, including APP/PS1 mu p75-SAP, APP/PS1 Sham, WT SAP and WT Sham mice.

Table

Acetyl Cholinesterase Activity in Wild-type and APP^{swe}/PS1^{E9} Mice Lesioned with Murine p75^{NTR} Saporin Immunotoxin

| | 3 months (acute) | | | 7 months (acute) | | | 3 months (long term) | | |
|--------------|--------------------------|---------------------------|---------------|-------------------------|--------------------------|---------------|--------------------------|-------------------------|-------------|
| | Cortex | Hippocampus | Striatum | Cortex | Hippocampus | Striatum | Cortex | Hippocampus | Striatum |
| APP/PS1 Sap | 61.32±5.18 ^{**} | 33.75±2.80 ^{**} | 86.0480±8.46 | 61.40±5.44 [*] | 62.32±6.32 ^{**} | 111.7445±4.92 | 63.36±5.26 ^{**} | 55.42±7.08 [*] | 84.74±8.22 |
| APP/PS1 Sham | 95.52±8.62 | 87.86±3.71 | 100.7733±6.82 | 81.10±6.40 | 81.26±6.91 | 97.9884±13.36 | 82.65±3.93 | 80.76±5.23 | 112.88±9.65 |
| Wt Sap | 67.49±1.91 ^{**} | 51.21±12.40 ^{**} | 92.2547±1.94 | 65.94±6.65 [*] | 65.83±6.97 ^{**} | 100.0001±6.58 | 60.86±6.93 ^{**} | 57.43±9.80 [*] | 88.67±10.20 |
| Wt Sham | 100.00±9.42 | 100.00±8.69 | 100.0072±4.51 | 100.00±6.90 | 100.00±5.02 | 102.8323±7.21 | 100.00±11.46 | 100.00±9.16 | 99.84±7.63 |

Data are expressed as percentage of Wt Sham values and are representative of 4–11 mice. Differences were detected with one-way ANOVA followed by Tukey-b or Tamhane tests as required. 3 months acute: Cortex [F(3, 16) = 7.401, ^{*}p = 0.003 vs. Wt Sham and APP/PS1 Sham], hippocampus [F(3, 15) = 18.801, ^{**}p < 0.001 vs. Wt Sham and APP/PS1 Sham], striatum [F(3, 16) = 1.12, p = 0.371]. 7 months acute: Cortex [F(3, 74) = 3.43, ^{*}p = 0.021 vs. Wt Sham and APP/PS1 Sham], hippocampus [F(3, 71) = 7.007, ^{**}p < 0.001 vs. Wt Sham and APP/PS1 Sham], striatum [F(3, 80) = 7.007, p = 0.791]. 7 months long-term: Cortex [F(3, 26) = 5.126, ^{**}p = 0.006 vs. Wt Sham and APP/PS1 Sham], hippocampus [F(3, 38) = 4.101, ^{*}p = 0.013 vs. Wt Sham and APP/PS1 Sham], striatum [F(3, 47) = 1.73, p = 0.172].